DOE/PC/79922--T5

DE91 002492

Twelfth Quarterly Report

CYCLONE PERFORMANCE AND OPTIMIZATION

US Department of Energy grant DE-FG22-87PC79922

submitted to:

U.S. Department of Energy
Pittsburgh Energy Technology Center
PO Box 10940
Pittsburgh, PA 15236

by:

David Leith
919 966-3851
Department of Environmental Sciences and Engineering
University of North Carolina
Chapel Hill, NC 27599

15 September 1990

Note: US/DOE Patent Clearance is <u>not</u> required prior to publication of this document

CYCLONE OPTIMIZATION BASED ON A NEW EMPIRICAL MODEL FOR PRESSURE DROP

G.Ramachandran, John Dirgo*, and David Leith

Department of Environmental Sciences and Engineering
University of North Carolina
Chapel Hill, NC 27599

*Planning Research Corporation
303 East Wacker Drive
Chicago, IL 60601

ABSTRACT

An empirical model for predicting pressure drop across a cyclone is developed through a statistical analysis of pressure drop data for 98 cyclone designs. The model is shown to perform better than the pressure drop models of First (1950), Alexander (1949), Barth (1956), Stairmand (1949), and Shepherd-Lapple (1940). This model is used with the efficiency model of Iozia and Leith (1990) to develop an optimization curve which predicts the minimum pressure drop and the dimension rations of the optimized cyclone for a given aerodynamic cut diameter, d_{50}. The effect of variation in cyclone height, cyclone diameter, and flow on the optimization curve is determined. The optimization results are used to develop a design procedure for optimized cyclones.

SUMMARY

The objectives of this project are: to characterize the gas flow pattern within cyclones, to revise the theory for cyclone performance on the basis of these findings, and to design and test cyclones whose dimensions have been optimized using revised performance theory. This work is important because its successful completion will aid in the technology for combustion of coal in pressurized, fluidized beds.

During the past quarter, we have (a) completed modeling work that employs the flow field measurements made during the past six months, (b) prepared a draft of a thesis based on these flow field measurements, and (c) prepared a paper for publication that combines a new model for pressure drop with our optimization procedure to allow a new design procedure for cyclones.

We have applied for a six month time extension to complete work on this project. During this time, we plan to complete two additional papers for publication. The first paper is attached as this quarter's technical progress report. The second paper will be based on the flow field measurements now completed. These will bring to five the number of journal articles submitted for publication under this project.

INTRODUCTION

Pressure drop and collection efficiency are the two major criteria used to evaluate cyclone performance. Both criteria are functions of cyclone dimensions: inlet height, a, inlet width, b, gas outlet diameter, D_e, outlet duct length, S, cylinder height, h, cyclone height, H, and dust outlet diameter, B; see Figure 1. The goal of cyclone design is to obtain the greatest efficiency for a given operating cost (pressure drop) by adjusting these dimensions.

Any design method based on theory depends on the accurate prediction of efficiency and pressure drop. Dirgo and Leith (1985) developed an optimization program to investigate design changes that would improve performance. Due to the poor prediction by the efficiency and pressure drop theories used (Barth, 1956; Leith-Licht, 1972; Stairmand, 1949), substantial improvement in performance was not shown by pilot scale cyclones designed according to the program. Thus, efficiency and pressure drop theories with better predictive capabilities are needed.

Subsequently, Iozia and Leith (1990) developed an improved method to predict cyclone aerodynamic cut diameter, d_{50}. Aerodynamic cut diameter is the particle size collected with 50 percent efficiency. Iozia and Leith claimed that their method works better than the theories of Lapple (1950), Leith-Licht (1972) and Dietz (1981). The equations necessary to use this model are in the Appendix.

Pressure drop models currently used include those by First (1950), Alexander (1949), Barth (1956), Stairmand (1949) and Shepherd-Lapple (1940). None of these predicts pressure drop accurately for a wide range of cyclone designs; predictions can differ from measured values by more than a factor of two (Dirgo, 1988). Further, evaluation of cyclone pressure drop models by different investigators have produced conflicting conclusions as to which models work best. Stern et al. (1955) found that the Shepherd-Lapple model provided the best fit to experimental data although for some cyclones the First and Alexander models worked equally well. Leith and Mehta (1973) found that the Barth, Stairmand, and Shepherd-Lapple models predicted results most accurately. They recommended the Shepherd-Lapple model because of its simplicity. In a later review based on a larger data set, Leith, Dirgo and Davis (1986) found that the Stairmand and Shepherd-Lapple models were most accurate. Kaplan (1977) recommended the Alexander model. This paper presents a new empirical model for predicting pressure drop. The model was developed through statistical analysis of pressure drop data for 98 cyclone designs, a substantially larger data set for evaluation of pressure drop models than has been used previously.

The present study uses the efficiency model of Iozia and Leith (1990) and the pressure drop model developed here to determine design changes that should optimize cyclone performance. Our goal was to design cyclones that provide the greatest efficiency (minimum d_{50}) for a given pressure drop.

PRESSURE DROP MODEL

Pressure drop, ΔP, will be expressed as the number of gas inlet velocity heads, ΔH. This dimensionless term is related to pressure drop in height of a column of a liquid, ΔP, by

$$\Delta P = \Delta H \, (v_i^2 \, \rho_G) \, / \, (2 \, \rho_L \, g) \qquad (1)$$

where ΔP is cyclone pressure drop (m of liquid), v_i is gas inlet velocity (m/s), ρ_G is gas density (kg/m^3), ρ_L is liquid density (kg/m^3) and g is the acceleration of gravity (m/s^2). ΔH is a function of the cyclone dimension ratios only and is not affected by operating conditions such as gas flow. ΔH should remain constant for any cyclone configuration, regardless of size, as long as the relative proportions of the dimensions stay the same.

We conducted a literature review to identify data that could be used to evaluate existing cyclone pressure drop models and to develop a better model. Decisions to include specific studies for this review were based on four criteria. Data were included only if all four criteria were met:

1. ΔH was presented or could be calculated from reported values of cyclone pressure drop, ΔP, and operating conditions.

2. All cyclone dimensions were presented or could be determined from drawings of known scale. For nine cyclones, all dimension ratios except the dust outlet diameter, B, could be determined by these methods. We assigned a value of 0.25 to B and included these cyclones in the study.

3. Sufficient information was presented so that ΔH could be calculated from the pressure drop models of Shepherd-Lapple, First, Barth, Stairmand, and Alexander.

4. The cyclone was similar in configuration to the reverse flow cyclone in Figure 1. Cyclones that were significantly different were excluded, e.g., cyclones with scroll-type inlets.

We found data for 98 cyclones that met these criteria. The seven dimension ratios, the reported ΔH for each cyclone, and the literature sources from which the data were obtained are in Table 1.

We developed a correlation matrix for these data to investigate the relationship between cyclone dimension ratios and ΔH. The matrix includes three dimension ratios in addition to the seven basic dimension ratios:

1. $(H\text{-}h)/D$, the ratio of cyclone cone length to cyclone diameter,

2. $(H\text{-}S)/D$, the ratio of cyclone core length to diameter; the core is defined as the distance from the bottom of the gas outlet duct to the dust outlet,

3. (ab/D_e^2), the ratio of the gas inlet area to the square of the gas outlet duct diameter; this term is proportional to the ratio of gas inlet to outlet area.

Table 2 is the correlation matrix for these dimension ratios and ΔH. SAS (1982) programs produced the correlation matrix and all subsequent statistical analyses. The correlation matrix shows that cyclone inlet $(a/D, b/D)$ and outlet (D_e/D) dimension ratios are most highly correlated with ΔH. When these ratios are combined as (ab/D_e^2), the correlation coefficient with ΔH is 0.976. The inlet and outlet dimension ratios are not strongly correlated with other cyclone dimension ratios, and none of the other dimension ratios is strongly correlated with ΔH. However, strong correlations exist among these other ratios, particularly for ratios that include cyclone height, H.

We used stepwise and backward regression to suggest possible models for ΔH based on cyclone dimension ratios (Draper and Smith, 1966). Both regressions used natural logarithms of ΔH and the dimension ratios to produce models of the form

$$\Delta H = K A^X B^Y C^Z \tag{2}$$

where K is a constant, and A, B, and C are cyclone dimension ratios.

We ran two sets of stepwise and backward regressions; each set investigated three possible models. The first set included the cyclone gas inlet and outlet dimension ratios, a/D, b/D, and D_e/D, independently. Each of the three models also included cylinder height, h/D, outlet duct length, S/D, and dust outlet diameter, B/D. The first model included cyclone height, H/D, the second included cone height, $(H\text{-}h)/D$, and the third core height $(H\text{-}S)/D$. We did not include these last three dimension ratios in the same model because they are highly correlated and as general measures of cyclone height, they are likely to explain the same variability in ΔH. The second set of three models was identical to the first set, except that cyclone gas inlet and outlet dimension ratios were grouped as (ab/D_e^2).

The stepwise and backward regression procedures produced identical results for all potential models investigated. In each case, the stepwise procedure included all dimension ratios in the model (seven dimension ratios for models using a, b, and D_e; five dimension ratios for models using (ab/D_e^2)). The backward procedure left all dimension ratios in the model. After reviewing these models, the following model was selected for further evaluation:

$$\Delta H = 19.7\,(ab/D_e^2)^{0.99}\,(S/D)^{0.35}\,(H/D)^{-0.34}\,(h/D)^{-0.35}\,(B/D)^{-0.33} \;. \tag{3}$$

The first three exponents in Eq. (3) are statistically significant at the $p < 0.003$ level based on partial F-test values; the exponent for B/D is significant at the $p = 0.006$ level. The coefficient of determination, R^2, for this model is 0.917. A major consideration in selecting Eq. (3) is that this model can be expressed in simpler form. Rounding off the constant and exponents, and combining secondary dimension ratios produces

$$\Delta H = 20\{ab/D_e^2\} \{[S/D]/[(H/D)(h/D)(B/D)]\}^{1/3} \quad (4)$$

Partial F-tests show that Eqs. (3) and (4) are not significantly different. We used Eq. (4) to predict ΔH values for the 98 cyclones in our data set. Figure 2 plots observed ΔH vs. the values predicted by Eq. (4).

Comparison of Eq. (4) with Other Pressure Drop Models

For each of the cyclones in our data set, we calculated the pressure drop values predicted by the Shepherd-Lapple (1940), First (1950), Barth (1956), Stairmand (1949), and Alexander (1949) models and also by Eq. (4). For each model, we calculated a geometric mean difference between the observed and predicted ΔH values,

$$\ln d_g = \sum_{i=1}^{n} (\ln \Delta H_{obs} - \ln \Delta H_{pred})/n \quad (5)$$

The geometric mean difference can be used to determine whether, on average, a model overestimates or underestimates ΔH. We also calculated a least squares performance index, I, for each model:

$$\ln d_g = \sum_{i=1}^{n} (\ln \Delta H_{obs} - \ln \Delta H_{pred})^2/n \ . \quad (6)$$

I is derived from the quantity minimized when a regression line is fitted to data by the method of least squares. The model with minimum value of I best fits the data.

Results of these analyses presented in Table 3 show that Eq. (4) performed better than the other five models; d_g was closest to one and I was lowest. These results were expected because Eq. (4) was developed from a least squares regression for the same ΔH values used for the inter-model comparison. Table 3 shows that Eq. (4) and the First and Barth models tended to predict ΔH values higher than those observed; d_g was less than one. The Shepherd-Lapple, Stairmand, and Alexander models tended to underestimate ΔH. The Alexander and Shepherd-Lapple models were the poorest predictors of ΔH.

We also looked at the accuracy of cyclone pressure drop models a second way. Table 4 shows the fraction of predictions for each model within 10, 20, and 30 percent of the observed ΔH. The results in Table 4 generally agree with the evaluation of models based on I; Eq. (4) performs best. For Eq. (4), over 40% of the predictions were within 10% of the observed ΔH; nearly 70% were within 20% of ΔH; over 80% were within 30% of ΔH. Table 4 also shows that the First model was more accurate than the Barth model. Since the First model is also much simpler, it should be preferred over the Barth model. These comparisons show that the number of cyclone dimension ratios included in a model is an important factor in predicting ΔH. The two models that performed much worse than the others, Alexander and Shepherd-Lapple, base their predictions on only the gas inlet and outlet dimension ratios, a/D, b/D, and D_e/D. The four models that predict ΔH much better include additional dimension ratios.

Although Eq. (4) is more accurate than existing pressure drop models, Figure 2 shows that this equation cannot predict ΔH accurately for all cyclone designs. Two factors may have contributed to differences between predicted and observed ΔH values. First, most literature sources did not report how pressure drop was measured. Some measurements may not have been corrected for differences in velocity pressure at the gas inlet and outlet. This would have affected reported ΔH values, particularly for cyclones with large differences in inlet and outlet cross-sectional areas. Second, most literature sources did not provide data on dust loading. Cyclone pressure drop decreases as dust concentrations increase (Stern et al., 1955; Tengbergen, 1965; Yuu et al., 1978); however, cyclone pressure drop models do not consider this effect. Model predictions could have overestimated ΔH for dust gas streams.

Cross-Validation

Testing Eq. (4) on the data from which it was developed will overestimate its performance. Cross-validation is one method of evaluating a model's predictive ability for new data (Mosteller and Tukey, 1977). This statistical procedure also helps to evaluate the form of a model, in this case, the dimension ratios used to predict ΔH, and the numerical values of the model's coefficients; i.e., the exponents for the dimension ratios. We carried out a simple cross-validation on the data set in Table 1. The data were randomly divided in half. We repeated the modeling procedure described above for half the data. The model was then tested on the other half.

The model that resulted from this analysis was very similar to the model developed from the full data set. The major difference between the cross-validation model and the full data set model was that the dust outlet diameter, B, was not included in the cross-validation model.

When tested on the second half of the data set, the cross-validation model performed better than most existing pressure drop models and nearly as well as the rest. However, when the entire data set was considered, the cross-validation model performed better than any of the existing models. Thus, Eq. (4), which is very similar to the cross-validation model, might also be expected to predict ΔH accurately for new cyclones.

OPTIMIZATION

Our goal was to predict dimension changes that would improve cyclone performance compared to a baseline defined by the Stairmand high efficiency cyclone. To do this, we used Eqs. (1) and (4) for pressure drop and the efficiency model of Iozia and Leith, the Appendix. Since the equation for efficiency, Eq. (A6), shows that efficiency can be maximized by minimizing d_{50}, the optimization procedure minimized d_{50} for a given pressure drop. The procedure (Dirgo and Leith, 1985; Iozia and Leith, 1989) used in this study is a variation of the single factor method (Cochran and Cox, 1957). Two cyclone dimensions were varied simultaneously. Gas outlet diameter, D_e, selected as the primary dimension, was varied first. This changed the pressure drop. Each of the six remaining dimensions was then varied, one at a time, to bring pressure drop back to the original value. Pressure drop was held constant because improvements in performance are difficult to evaluate if pressure drop changes. The d_{50} for each new design was then predicted from theory. The new design with lowest d_{50} became the baseline for the next iteration. In the next iteration, the gas outlet diameter, D_e, was again varied in a pairwise fashion with each of the six other dimensions to find the second dimension change that most reduced d_{50} while keeping pressure drop constant. Iterations were continued until the predicted reduction in d_{50} from iteration to iteration was less than one nanometer.

Some dimensions were subject to constraints. The optimization program would increase dust outlet diameter, B, until it equalled the cyclone diameter. However, in this work, B as set equal to 0.375 D to bring the collected dust to a central point. The cylinder height, h, was set equal to 1.5 D so that cyclone height varied by changing cone height, H-h.

Optimization was done for 40 pressure drops from 0.1 kPa to 4.0 kPa in steps of 0.1 kPa. Thus, for operation over this ΔP range, we determined cyclone designs that would give the lowest d_{50} possible according to the models used for efficiency and pressure drop.

RESULTS AND DISCUSSION

Figure 3 shows the relationship between predicted pressure drop and predicted aerodynamic d_{50} for optimized designs. It indicates the predicted optimum performance for cyclones. The area above the line indicates current practice. To show this, predicted performance for selected cyclone designs from the experimental work of Lapple (1950), Peterson and Whitby (1965), Dirgo and Leith (1985) and Iozia and Leith (1990) are shown. The relationship shows a trade-off between efficiency and operating cost. Greater efficiency (lower d_{50}) requires greater operating cost (pressure drop).

Figure 4 shows how inlet height, a, inlet width, b, and outlet diameter, D_e, varied with aerodynamic d_{50}. A program constraint was that $b < (D - D_e)/2$ to prevent "crowding" of the entering gas. At $b \geq 0.2\,D$, this limit was achieved, for $D_e = 0.6\,D$, resulting in a flat curve for b for $d_{50} \geq 3$ µm. In this region, inlet height was increased to achieve higher d_{50} cuts. Inlet width and outlet diameter were relatively constant regardless of d_{50}, and so were largely independent of pressure drop. Gas outlet duct length, S, was always found equal to inlet height.

For optimized designs at all pressure drops, the outlet area, πD_e^2, was larger than inlet area, ab. Thus the inlet velocity head is greater than the outlet velocity head. This leads to a lower pressure drop across the cyclone than if the inlet and outlet areas were equal.

Figure 5 shows pressure drop vs. aerodynamic d_{50} for $H = 4D, 5D$, and $6D$. For any pressure drop, increases in cyclone height, H, decrease d_{50}. An explanation for this can be obtained from the "static particle" theory. According to this theory, the particle with diameter d_{50}, called the critical particle, remains suspended within the cyclone due to the balance of centrifugal and radial drag forces. The radial drag force depends on the average radial velocity of gas, V_r, flowing inward past the critical particle. V_r is given by

$$V_r = Q / (2 \pi r_c z_c) \tag{7}$$

where Q is the gas flow, r_c is the core radius, and z_c is the core length (Barth, 1956). Core length, z_c, is directly proportional to cyclone height, H. An increase in H will increase z_c, thereby reducing V_r and hence the drag force. Thus, as H increases, a smaller d_{50} particle can be balanced on the edge of the core.

Another way to view Figure 5 is that for any d_{50}, increases in cyclone height reduce pressure drop. First (1949) suggested that a shorter cone causes the gas outlet opening to function as a valve. Gas is diverted from the downward flowing outer vortex to the upward flowing inner vortex at a faster rate than it can enter the exit duct. This causes a secondary downward flow within the inner vortex, increasing pressure drop. A longer cyclone would reduce this effect.

Figure 6 shows how inlet height, a, inlet width, b, and outlet diameter, D_e, varied with aerodynamic d_{50} for cyclones of each height. This figure shows that D_e and b do not change with changes in H but inlet height, a, increases with H. This is consistent with the observation that b and D_e are independent of pressure drop and hence are also independent of H.

Figure 7 shows pressure drop vs. aerodynamic d_{50} for different flows through the cyclone. It illustrates a trade-off between flow and d_{50}. For a particular operating cost (pressure drop) as flow increases, efficiency decreases. Figure 8 shows that an increase in flow is accompanied by an increase in inlet height, a. Inlet width and outlet diameter do not change significantly with flow.

This can be understood by substituting Eqs. (A2) and (A5) from the Appendix into Eq. (A1) to obtain

$$d_{50} \approx (9\,\mu/(\pi\,\rho_p\,z_c))^{1/2}(1/6.1)\,(1/Q)^{1/2}\,(a^{0.39}\,b^{0.39}\,D^{0.15}\,D_e^{0.74}\,H^{0.33})\ . \tag{8}$$

D_e and b are roughly constant. H and D are kept constant. If Q increases, then a must increase to keep d_{50} the same. From Eqs.(1) and (4), an increase in inlet height will increase pressure drop as can be seen in Figures 7 and 8.

Figure 9 shows pressure drop vs. aerodynamic d_{50} for different cyclone diameters. It shows that as cyclone diameter, D, increases, pressure drop (operating cost) decreases. Cyclone capital costs are proportional to surface area and are therefore proportional to D^2. Thus, if capital costs increase, operating costs decrease. The designer must strike a balance between the higher capital cost that a bigger cyclone entails and the lower operating cost it brings.

Figure 10 shows that an increase in cyclone diameter is accompanied by a decrease in inlet height, a. This again can be understood by referring to Eq. (8). If D increases, then since b and D_e are almost constant and H and Q are constant, a must decrease to keep d_{50} constant. From Eq. (4), a decrease in a will decrease pressure drop.

ENGINEERING DESIGN

For any application, the required overall collection efficiency is first specified. A d_{50} is then selected in the following way. The particle size distribution of the dust must be known. Let $c_1, c_2, ..., c_N$ be the fraction of particles in each size range. A value of d_{50} is chosen arbitrarily. For each size range, the collection efficiency is calculated from Eq. (A6) as $\eta_1, \eta_2, ..., \eta_N$. The overall efficiency is then calculated as

$$\eta_{overall} = c_1\,\eta_1 + c_2\,\eta_2 + ... + c_N\,\eta_N. \tag{9}$$

If the required overall efficiency is greater than the calculated overall efficiency, then d_{50} is decreased, and this process is repeated. By trial and error a value of d_{50} is found such that the required overall efficiency is obtained. This d_{50} is located on the optimization curve of Figure 5. The pressure drop, ΔP, corresponding to this d_{50} is found. Cyclone inlet height, a, width, b, and outlet diameter, D_e, are found from the dimension ratios of Figure 6 for the specified d_{50}. Cyclone diameter, D_2, is found by

$$D_2 = D_1\,(\rho_{p2}\,Q_2/\,\rho_{p1}\,Q_1)^{1/3} \tag{10}$$

after Stairmand (1951), where D_1, ρ_{p1}, and Q_1 are the cyclone diameter (25.4 cm), particle density (1 g/cm^3) and flow (0.94 m^3/s) of the cyclone optimized in Figure 6, and ρ_{p2} and Q_2 are the corresponding values for the system being designed. Design pressure drop, ΔP_2, is found according to

$$\Delta P_2 = \Delta P_1 \left(Q_2 D_1^2 / Q_1 D_2^2 \right)^2 , \tag{11}$$

where ΔP_1 is the pressure drop from Figure 5 corresponding to the constant d_{50}; Q_1 and D_1 are the flow and cyclone diameter of the optimization curve (Iozia and Leith, 1989). Q_2 and D_2 are the flow and cyclone diameter of the system to be designed. D_2 is obtained from Eq. (10).

If the pressure drop, ΔP_2, is too high, then the designer should explore other alternatives. A taller cyclone can be chosen as the starting point and the design procedure described above can be repeated. However, a tall cyclone may not always be feasible, especially if it is to be installed at an indoor location with space constraints. A larger diameter can be chosen as the starting point of the design. This would lower pressure drop but increase capital costs. Another way to lower pressure drop would be to reduce flow through the cyclone. This would mean installing additional cyclones in parallel, leading to higher capital costs. Thus every choice presents a trade-off to the designer.

CONCLUSIONS

In this work, a new empirical model for predicting pressure drop across a cyclone was developed. This model is based on statistical analysis of cyclone data and does not add to fundamental understanding of cyclone mechanics. The model also does not take into account the effect of inlet dust loading on cyclone performance. Despite these shortcomings, this model seems capable of better predictions than other models.

Using this model and the efficiency model of Iozia and Leith (1989), an optimization curve was developed which predicted the minimum pressure drop and the dimension ratios of the optimized cyclone for a give d_{50}. The effect of variation in cyclone height, H, diameter, D, and flow, Q, on the optimization curves was determined.

The optimization curves were used to develop a design procedure for optimized cyclones. The procedure shows that for any set of design criteria, several optimized cyclones may be used. Each of these presents a trade-off that must be made. The designer must choose the alternative most economically feasible.

ACKNOWLEDGEMENT

This material was prepared with the support of the U.S. Department of Energy, Grant DE-FG22-87PC9922. Any opinions, findings, conclusions, or recommendations expressed herein are those of the authors and do not necessarily reflect the views of DOE.

REFERENCES

Alexander R. Mc.K. (1949). *Proc. Australas. Inst. Min. Met. (New Series).* 152-3: 203.

Barth, W. (1956). *Brennstoff-Warme-Kraft*. 8: 1.

Cochran, W.G. and Cox, G.M. (1957). *Experimental Designs*. Second edition. 354. John Wiley and Sons, Inc., New York.

Dietz, P.W. (1981). *A.I.Ch.E. Journal*. 27: 288.

Dirgo, J.A. and Leith, D. (1985). *Aerosol Science and Technology*. 4: 401.

Dirgo, J.A. and Leith, D. (1985). *Filtration and Separation*. 22: 119.

Dirgo, J. (1988). *Relationships Between Cyclone Dimensions and Performance*. Doctoral Thesis, Harvard University.

Draper, N.R. and Smith, H. (1966). *Applied Regression Analysis*. John Wiley and Sons Inc., New York.

Ernst, M., Hoke, R.C., Siminski, V.J., McCain, J.D., Parker, R. and Drehmel, D.C. (1980). in *Second Symposium on the Transfer and Utilization of Particulate Control Technology*, Vol. 4, EPA-600/9-80-039d, USEPA, RPT, NC.

First, M.W. (1949). Paper No. 49-A-127. *American Society of Mechanical Engineers Annual Meeting*.

First, M.W. (1950). *Fundamental Factors in Design of Cyclone Dust Collectors*. Doctoral Thesis, Harvard University.

Green, G.G., Hall, J.A. (1984). *Ann. Rev. Psychol*. 35: 37.

Hejma, J. (1971). *Staub-Reinhalt. Luft*. 37 (7): 22.

Iozia, D.L. and Leith, D. (1990). *Aerosol Science and Technology*. 12: 598.

Iozia, D.L. and Leith, D. (1989). *Filtration and Separation*. 26: 272.

Kalmykov, A.V., Afanasev, Y.M., and Shipunov, N.G. (1976). *Thermal Eng*. 22: 70.

Kaplan, K.J. (1977). Chpt. 3 in *Air Pollution*, 3rd ed., Vol. IV, Stern, A.C., ed., Academic Press, NY.

Lapple, C.E. (1950). *Industrial Hygiene Quarterly*. 11: 40.

Leineweber, L. (1967). *Staub-Reinhalt. Luft*. 27 (3): 1.

Leith, D. and Licht, W. (1972) *A.I.Ch.E. Symp. Ser.* 68: 196.

Leith, D. and Mehta, D. (1973). *Atmos. Environ.* 7: 527.

Leith, D., Dirgo, J., Davis, W.T. (1986). Chpt 6 in *Air Pollution*, 3rd ed., Vol. IV, Stern, A.C., ed., Academic Press, NY.

Louis, T.A., Fineberg, H.V., Mosteller, F. (1985). *Ann. Rev. Public Health*. 6: 1.

Mosteller, F. and Air Pollution, Tukey, J.W. (1977). *Data Analysis and Regression*. Addison-Wesley, Reading, MA.

Parker, J., Jain, R., Calvert, S., Drehmel, D. and Abbott, J. (1981). *Environ. Sci. Technol.* 15: 451.

Peterson, C.M. and Whitby, K.T. (1965). *ASHRAE J.* 7: 42.

Petroll, J. and Langhammer, K. (1962). *Freiberger Forschungsh.* A220: 175,

Petroll, J., Quitter, V., Schade, G. and Zimmermann, L. (1967). *Staub-Reinhalt. Luft.* 27 (3): 1.

Ranz, W.E. (1985). *Aerosol Science and Technology*. 4: 417.

SAS (1982). *User's Guide: Statistics*. SAS Institute, Cary, NC.

Shepherd, C.B. and Lapple, C.E. (1940). *Ind. Eng. Chem.* 32: 1246.

Stairmand, C.J. (1949). *Engineering*. 168: 409.

Stairmand, C.J. (1951) *Trans. Instn. Chem. Engrs.* 29: 356.

Stern, A.C., Kaplan, K.J., Bush, P.D. (1955). *Cyclone Dust Collectors*, American Petroleum Institute, New York, NY.

Swift, P. (1969). *Steam Heat. Eng.* 38: 453.

van Ebbenhorst Tengbergen, H.J. (1965). *Staub-Reinhalt. Luft.* 25 (11): 44.

Yuu, S., Jotaki, T., Tomita, Y. and Yoshida, K. (1978). *Chem. Eng. Sci.* 33: 1573.

APPENDIX

EQUATIONS FOR PREDICTING d_{50}, IOZIA AND LEITH (1989)

$$d_{50} = \{(9 \mu Q) / (\pi \rho_p z_c V_{tmax}^2)\}^{1/2} \quad \text{(A1)}$$

where μ = viscosity of gas
Q = flow through cyclone
ρ_p = density of particle

$$V_{tmax} = 6.1 V_i (ab/D^2)^{0.61} (D_e/D)^{-0.74} (H/D)^{-0.33} \quad \text{(A2)}$$

$$z_c = (H - S) \quad \text{for } d_c < B$$

$$= (H - S) - \{(H - S) / (D/B - 1)\} \{d_c/B - 1\} \quad \text{for } d_c > B \quad \text{(A3)}$$

$$d_c = 0.47 D (ab/D^2)^{-0.25} (D_e/d)^{1.4} \quad \text{(A4)}$$

$$V_i = Q/(ab) \quad \text{(A5)}$$

$$\eta = 1/(1 + (d_{50}/d)^{\beta}) \quad \text{(A6)}$$

$$\ln(\beta) = 0.62 - 0.87 \ln(d_{50}(cm)) + 5.21 \ln(ab/D^2) + 1.05 (\ln(ab/D^2))^2 \quad \text{(A7)}$$

FIGURE CAPTIONS

Figure 1. Reverse flow cyclone.

Figure 2. Observed ΔH vs. predicted ΔH for Eq. (4).

Figure 3. Optimum pressure drop, ΔP, vs. d_{50} for $H = 5D$ with experimental data.

Figure 4. Optimum dimension ratios vs. d_{50} for $H = 5D$.

Figure 5. Effect of variation in H on optimum pressure drop.

Figure 6. Effect of variation in H on optimum dimension ratios.

Figure 7. Effect of variation in Q on optimum pressure drop.

Figure 8. Effect of variation in Q on optimum dimension ratios.

Figure 9. Effect of variation in D on Optimum Pressure Drop.

Figure 10. Effect of variation in D on optimum dimension ratios.

TABLE 1
Reported Values for Cyclone Dimension Ratios and Pressure Drop (in Inlet Velocity Heads)

Source	D_e	a	b	S	H	h	B	ΔH
26	0.500	0.533	0.233	1.600	4.267	2.133	0.267	7.2
26	0.500	0.533	0.156	1.600	4.267	2.133	0.267	4.7
26	0.500	0.533	0.111	1.600	4.267	2.133	0.267	3.7
5	0.313	0.500	0.148	0.500	2.375	1.625	0.313	11.3
5	0.500	0.500	0.148	0.500	2.375	1.625	0.313	5.1
5	0.313	1.000	0.250	0.500	1.688	1.125	0.313	40.2
5	0.500	1.000	0.250	0.500	1.688	1.125	0.313	14.5
5	0.500	0.250	0.125	1.500	4.000	2.000	0.250	3.5
5	0.500	0.500	0.250	1.500	4.000	2.000	0.250	5.7
5	0.500	0.600	0.250	1.500	4.000	2.000	0.250	10.7
5	0.500	0.500	0.250	1.500	4.000	2.000	0.250	6.5
5	0.333	0.667	0.133	0.400	1.967	1.133	0.250	11.5
5	0.250	0.367	0.117	0.733	2.200	0.950	0.250	12.7
21	0.500	0.283	0.150	0.600	1.450	0.700	0.200	4.9
21	0.500	0.288	0.151	0.613	1.463	0.700	0.200	5.0
21	0.500	0.293	0.150	0.600	1.475	0.700	0.200	5.0
21	0.500	0.283	0.067	0.600	1.450	0.700	0.200	2.5
21	0.500	0.142	0.150	0.600	1.450	0.700	0.200	2.8
21	0.667	0.283	0.150	0.600	1.450	0.700	0.200	3.1
21	0.333	0.283	0.067	0.600	1.450	0.700	0.200	6.0
21	0.500	0.283	0.150	0.600	1.158	0.700	0.200	5.5
27	0.500	0.283	0.094	0.600	1.158	0.700	0.200	3.8
27	0.667	0.283	0.094	0.600	1.158	0.700	0.200	2.3
27	0.333	0.283	0.150	0.600	1.158	0.700	0.200	11.8
27	0.667	0.283	0.150	0.600	1.158	0.700	0.200	3.3
27	0.333	0.283	0.150	0.600	1.450	0.700	0.200	10.5
27	0.500	0.113	0.150	0.600	1.450	0.700	0.200	2.3
27	0.500	0.208	0.150	0.600	1.450	0.700	0.200	3.9
27	0.500	0.283	0.094	0.600	1.450	0.700	0.200	3.5
27	0.333	0.283	0.067	0.400	1.450	0.700	0.200	6.2
27	0.417	0.292	0.208	0.556	2.056	0.667	0.140	9.5
27	0.476	0.393	0.119	0.667	1.607	0.655	0.141	5.3
22	0.500	0.500	0.200	0.500	4.000	1.500	0.375	5.3
9	0.500	0.620	0.230	1.170	3.180	1.330	0.250	3.7
9	0.573	0.667	0.333	0.893	3.280	1.307	0.250	6.2

Source	D_e	a	b	S	H	h	B	ΔH
9	0.564	0.609	0.318	0.909	2.727	1.364	0.250	7.3
28	0.513	0.561	0.211	0.763	2.666	0.561	0.531	2.3
28	0.434	0.526	0.156	0.632	3.579	0.632	0.316	4.7
28	0.435	0.538	0.162	0.673	3.373	0.681	0.404	4.6
28	0.400	0.527	0.149	0.636	2.909	0.636	0.345	4.9
17	0.405	0.486	0.268	0.568	2.335	0.649	0.405	12.0
17	0.300	0.267	0.267	0.390	2.486	0.501	0.300	25.0
29	0.500	0.900	0.100	0.967	2.217	1.035	0.500	9.6
29	0.500	0.900	0.100	0.967	3.467	1.035	0.500	8.5
29	0.500	0.900	0.100	0.967	5.967	1.035	0.500	6.9
29	0.500	0.900	0.100	0.967	10.970	1.035	0.500	5.2
29	0.500	0.900	0.200	0.967	2.217	1.035	0.500	14.4
29	0.500	0.900	0.200	0.967	3.467	1.035	0.500	13.2
29	0.500	0.900	0.200	0.967	5.967	1.035	0.500	11.4
29	0.500	0.900	0.200	0.967	10.970	1.035	0.500	9.1
29	0.500	0.900	0.300	0.967	2.217	1.035	0.500	19.3
29	0.500	0.900	0.300	0.967	3.467	1.035	0.500	17.5
29	0.500	0.900	0.300	0.967	5.967	1.035	0.500	15.5
29	0.500	0.900	0.300	0.967	10.970	1.035	0.500	13.1
29	0.500	0.900	0.400	0.967	2.217	1.035	0.500	25.2
29	0.500	0.900	0.400	0.967	3.467	1.035	0.500	21.9
29	0.500	0.900	0.400	0.967	5.967	1.035	0.500	18.9
29	0.500	0.900	0.400	0.967	10.970	1.035	0.500	16.6
29	0.333	0.900	0.100	0.967	1.801	1.035	0.333	24.1
29	0.333	0.900	0.100	0.967	2.634	1.035	0.333	19.0
29	0.333	0.900	0.100	0.967	4.301	1.035	0.333	16.0
29	0.333	0.900	0.200	0.967	1.801	1.035	0.333	40.0
29	0.333	0.900	0.200	0.967	2.634	1.035	0.333	34.4
29	0.333	0.900	0.200	0.967	4.301	1.035	0.333	29.7
29	0.333	0.900	0.300	0.967	1.801	1.035	0.333	56.7
29	0.333	0.900	0.300	0.967	2.634	1.035	0.333	49.9
29	0.333	0.900	0.300	0.967	4.301	1.035	0.333	43.5
29	0.333	0.900	0.400	0.967	1.801	1.035	0.333	73.5
29	0.333	0.900	0.400	0.967	2.634	1.035	0.333	65.3
29	0.333	0.900	0.400	0.967	4.301	1.035	0.333	58.4
29	0.250	0.900	0.100	0.967	1.592	1.035	0.250	49.1
29	0.250	0.900	0.100	0.967	2.217	1.035	0.250	41.4
29	0.250	0.900	0.100	0.967	3.467	1.035	0.250	33.9
29	0.250	0.900	0.200	0.967	1.592	1.035	0.250	80.8
29	0.250	0.900	0.200	0.967	2.217	1.035	0.250	77.2

Source	D_e	a	b	S	H	h	B	ΔH
29	0.250	0.900	0.200	0.967	3.467	1.035	0.250	66.9
29	0.250	0.900	0.300	0.967	1.592	1.035	0.250	121.4
29	0.250	0.900	0.300	0.967	2.217	1.035	0.250	110.6
29	0.250	0.900	0.300	0.967	3.467	1.035	0.250	98.0
29	0.250	0.900	0.400	0.967	1.592	1.035	0.250	155.3
29	0.250	0.900	0.400	0.967	2.217	1.035	0.250	148.3
29	0.250	0.900	0.400	0.967	3.467	1.035	0.250	136.8
30	0.433	0.555	0.162	0.543	3.263	0.684	0.384	6.4
30	0.431	0.553	0.161	0.552	3.245	0.681	0.383	7.3
30	0.432	0.553	0.161	0.561	3.255	0.682	0.382	7.8
31	0.400	0.440	0.210	0.500	3.900	1.400	0.400	9.2
31	0.500	0.500	0.250	0.600	3.750	1.750	0.400	7.6
32	0.541	0.557	0.331	0.962	5.939	3.350	0.287	8.8
33	0.575	0.575	0.230	0.584	3.510	0.750	0.480	10.0
33	0.575	0.573	0.223	0.580	3.460	0.750	0.477	7.0
18	0.514	0.372	0.186	0.541	2.095	0.743	0.253	2.8
34	0.407	0.494	0.247	0.740	3.961	2.662	0.586	2.3
35	0.313	0.375	0.188	1.125	4.313	1.813	0.375	9.1
2	0.500	0.500	0.200	0.500	4.000	1.500	0.375	5.8
2	0.333	0.500	0.300	0.558	6.000	3.500	0.375	11.2
2	0.583	0.375	0.200	3.052	6.000	3.500	1.000	2.9
2	0.583	0.375	0.200	2.865	6.000	3.500	0.688	2.9
2	0.333	0.500	0.300	2.073	6.000	3.500	1.000	12.2

TABLE 2

Correlation Matrix for Cyclone Dimension Ratios and ΔH

	D_e/D	a/D	b/D	S/D	H/D	h/D	B/D	(H-h)/D	(H-S)/D	ab/D_e^2	ΔH
D_e/D	---										
a/D	-0.378	---									
b/D	-0.121	0.442	---								
S/D	0.092	0.148	0.171	---							
H/D	0.190	0.289	0.240	0.378	---						
h/D	0.096	-0.052	0.195	0.685	0.393	---					
B/D	0.199	0.271	0.244	0.528	0.557	0.473	---				
(H-h)/D	0.172	0.331	0.192	0.171	0.947	0.078	0.439	---			
(H-S)/D	0.181	0.274	0.217	0.184	0.980	0.269	0.476	0.969	---		
(ab/D_e^2)	-0.661	0.607	0.632	0.085	-0.051	-0.046	-0.073	-0.040	-0.073	---	
ΔH	-0.668	0.540	0.511	0.063	-0.156	-0.113	-0.165	-0.129	-0.179	0.976	---

Table 3
Geometric Mean Differences and Least Squares Performance Index for Cyclone Pressure Drop Models

Model	Geometric Mean Difference, d_g	Least Squares Performance Index, I
Shepherd-Lapple (1940)	1.165	0.229
First (1950)	0.922	0.129
Barth (1956)	0.957	0.121
Stairmand (1949)	1.180	0.149
Alexander (1949)	1.386	0.321
Eq. (4)	0.977	0.102

Table 4

Fraction of Predictions Within 10, 20 and 30 Percent of Observed ΔH for Cyclone Pressure Drop Models

Model	Fraction Within 10 Percent	Fraction Within 20 Percent	Fraction Within 30 Percent
Shepherd-Lapple (1940)	0.17	0.33	0.45
First (1950)	0.38	0.63	0.78
Barth (1956)	0.15	0.52	0.70
Stairmand (1949)	0.25	0.38	0.55
Alexander (1949)	0.15	0.27	0.37
Eq. (4)	0.41	0.66	0.81

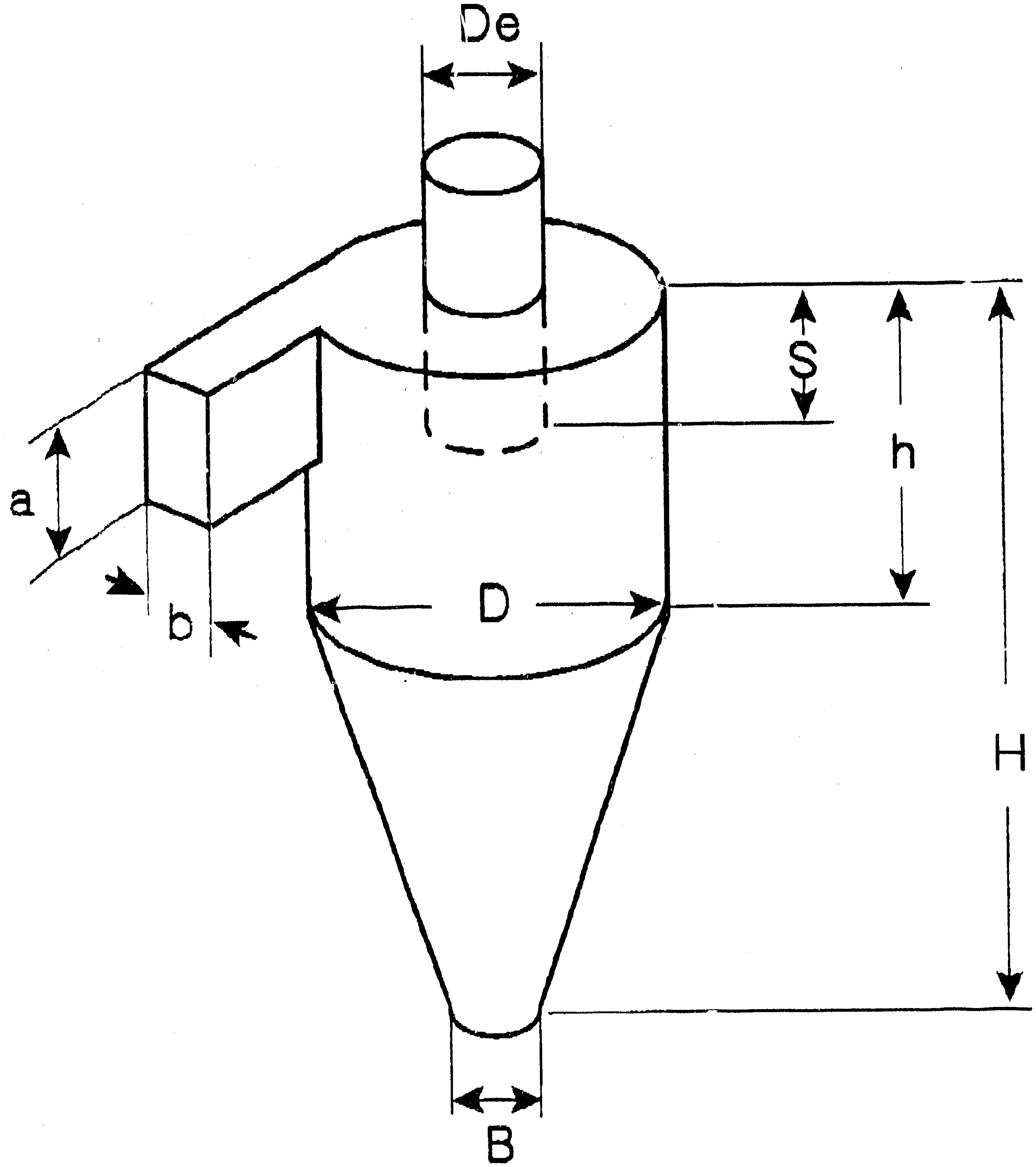

Figure 1

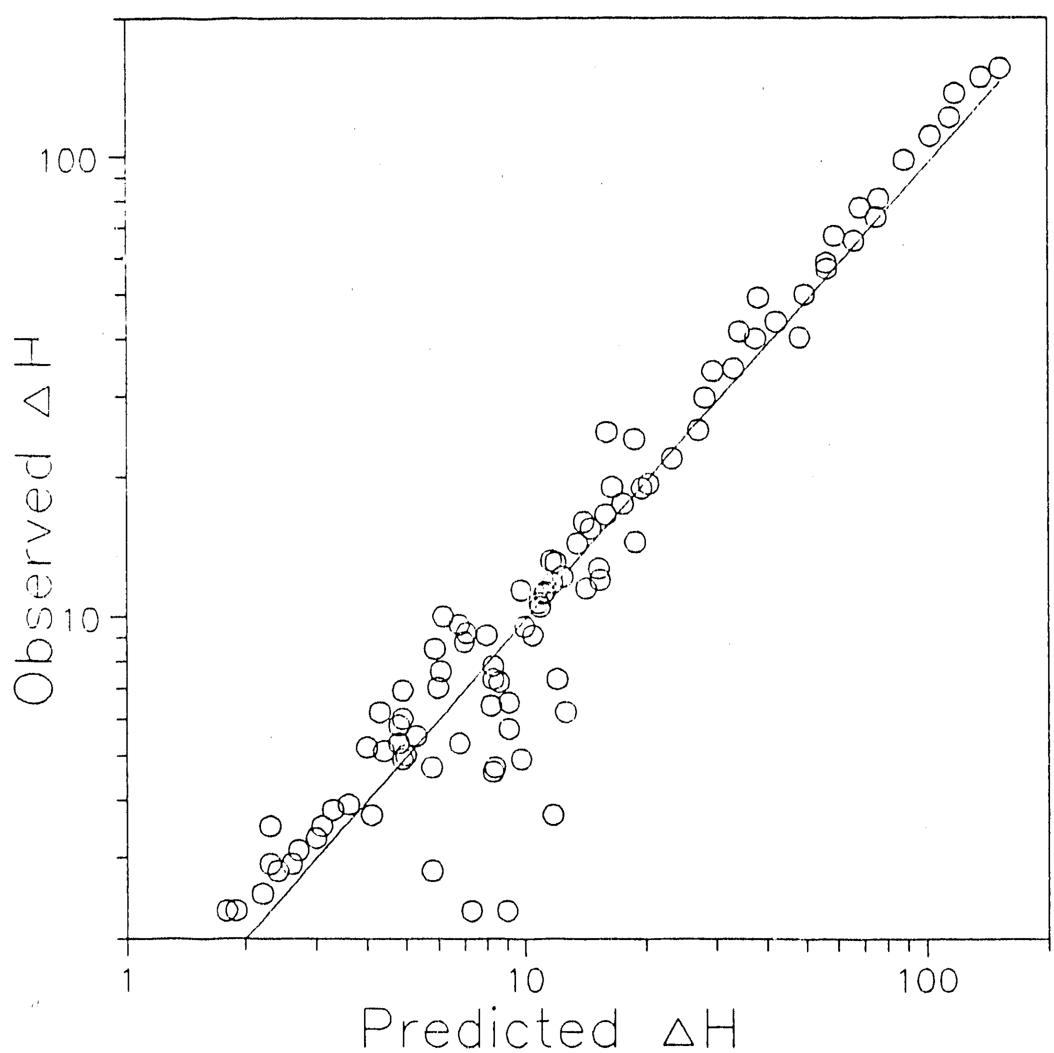

Figure 2

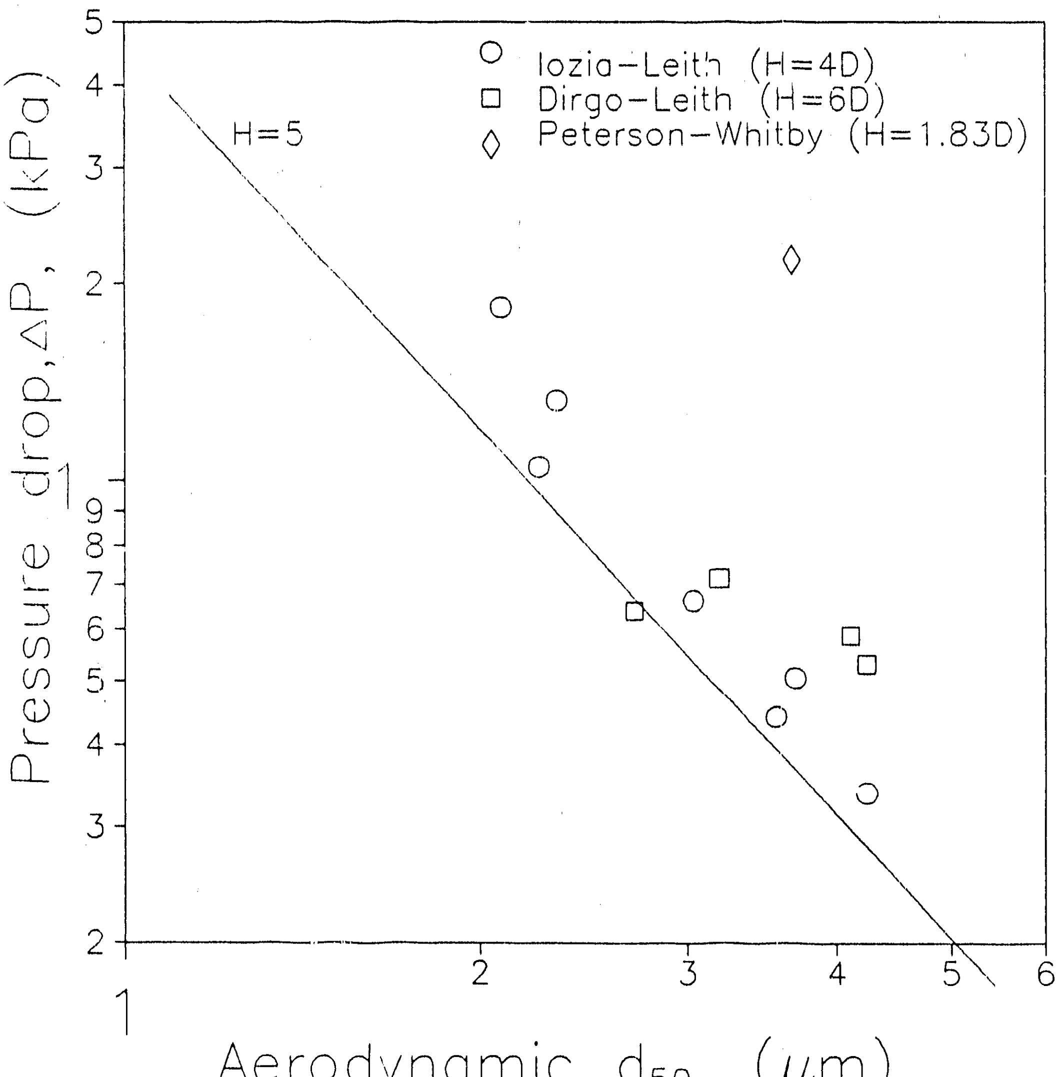
Iozia−Leith (H=4D)
Dirgo−Leith (H=6D)
Peterson−Whitby (H=1.83D)
H=5
Pressure drop, ΔP, (kPa)
Aerodynamic d50, (μm)
5
4
3
2
1
9
8
7
6
5
4
3
2
1
2
3
4
5
6

Figure 3

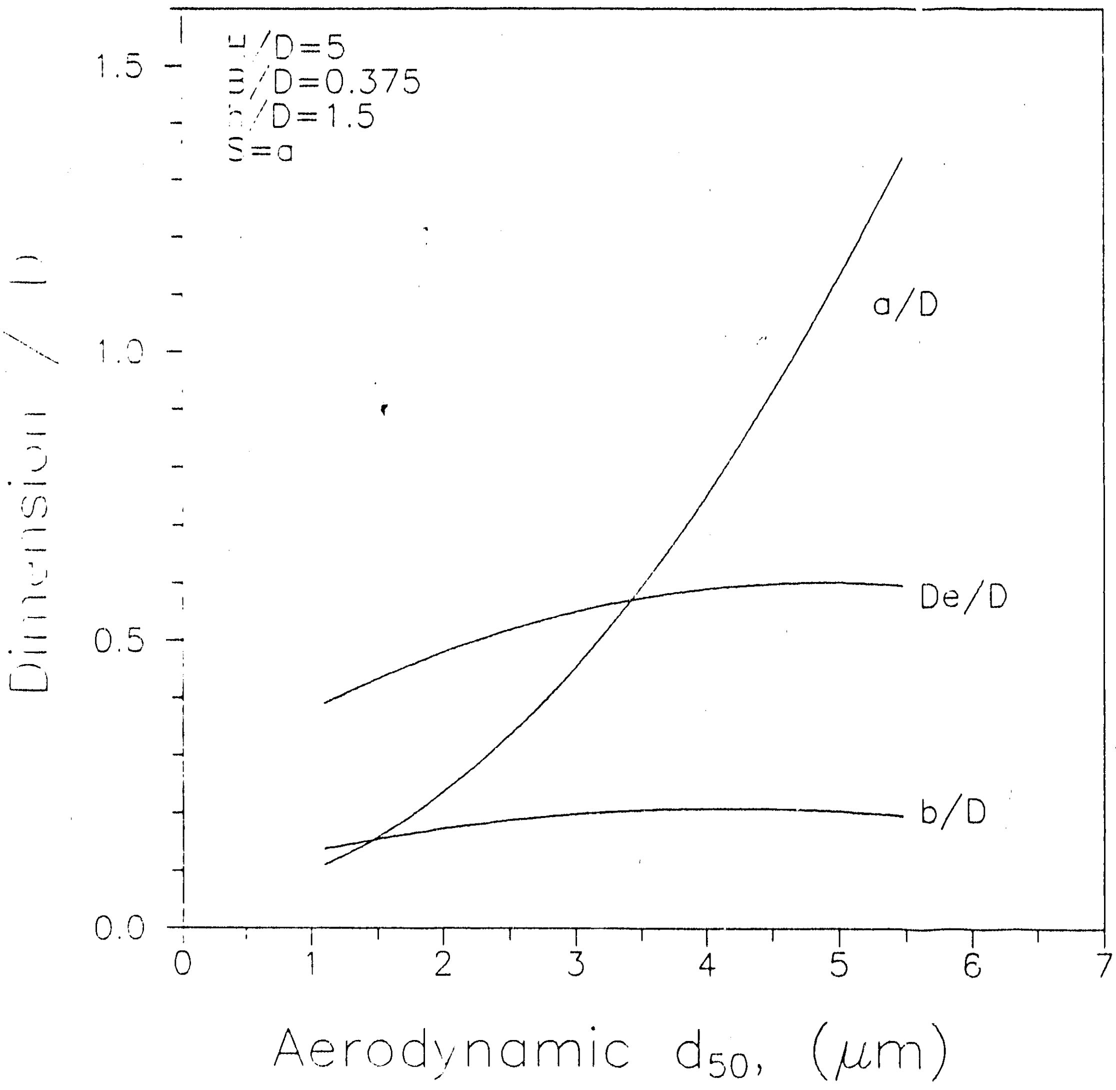
/D=5
B/D=0.375
/D=1.5
S=a
a/D
De/D
b/D
1.5
1.0
0.5
0.0
0
1
2
3
4
5
6
7
Dimension / D
Aerodynamic d50, (μm)

Figure 4

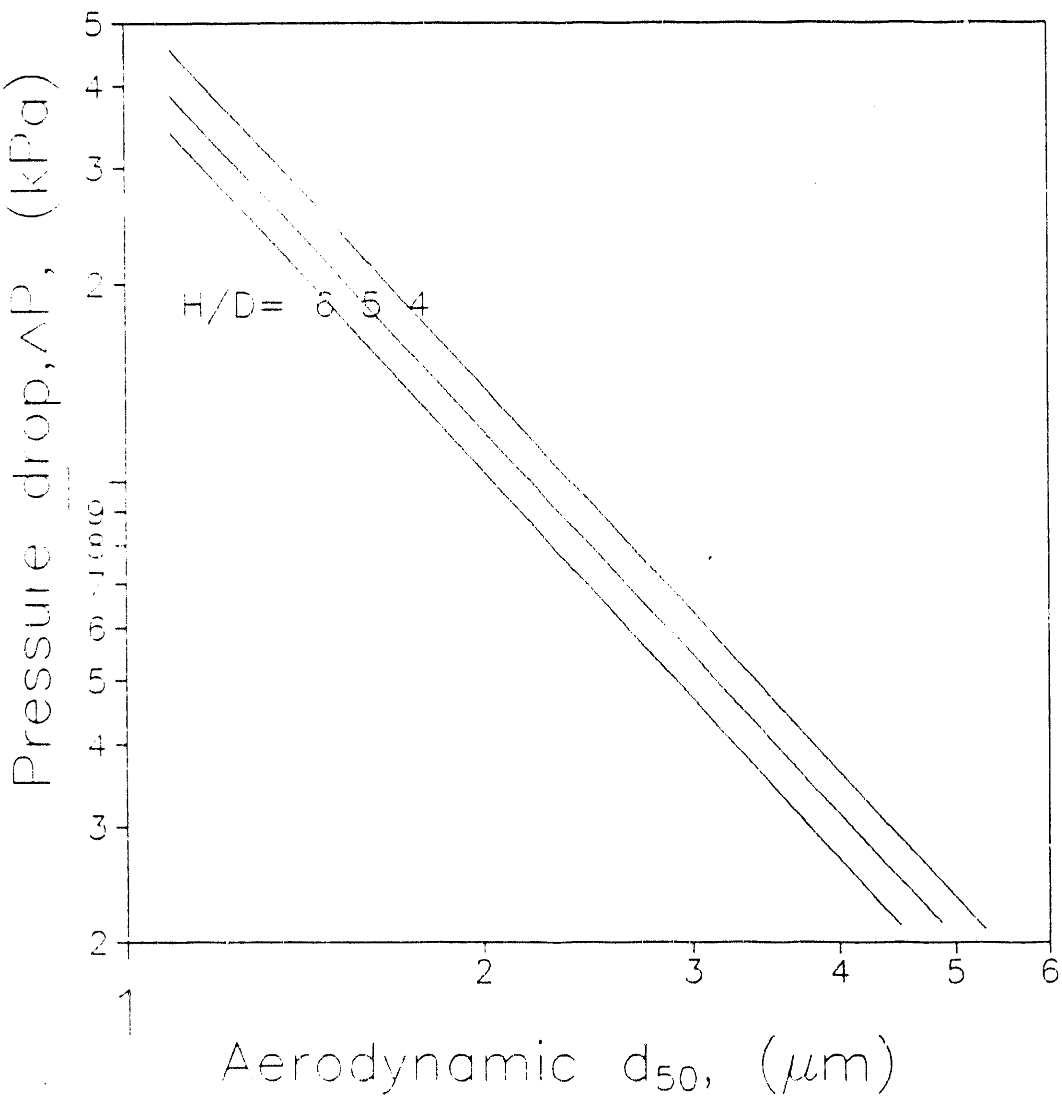
Pressure drop, ΔP, (kPa)
H/D= 6 5 4
Aerodynamic d50, (μm)
5
4
3
2
6
5
4
3
2
1
2
3
4
5
6

Figure 5.

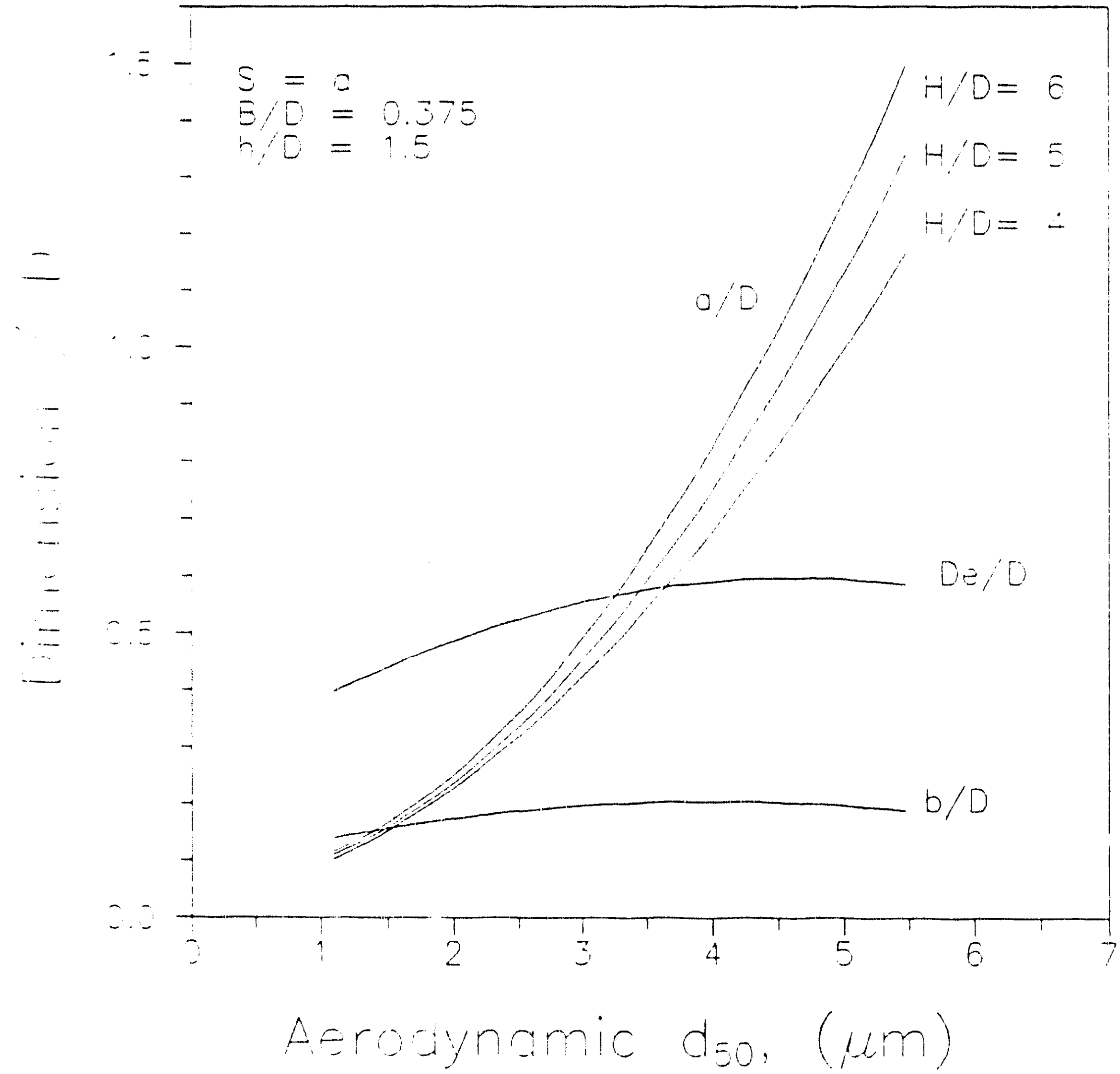

Figure 6.

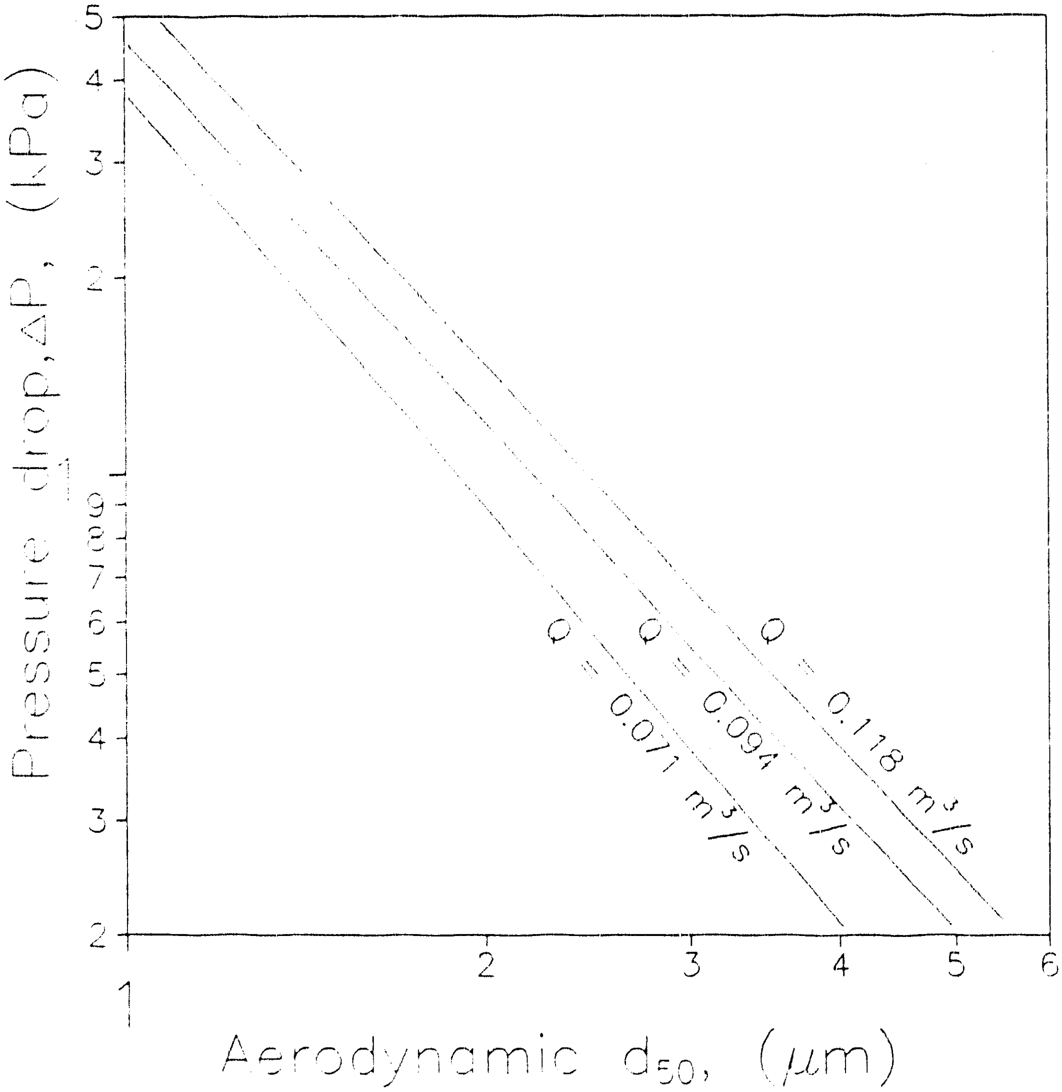
Pressure drop, ΔP, (kPa)
Aerodynamic d50, (μm)
Q = 0.071 m3/s
Q = 0.094 m3/s
Q = 0.118 m3/s
5
4
3
2
1
9
8
7
6
5
4
3
2
1
2
3
4
5
6

Figure 7.

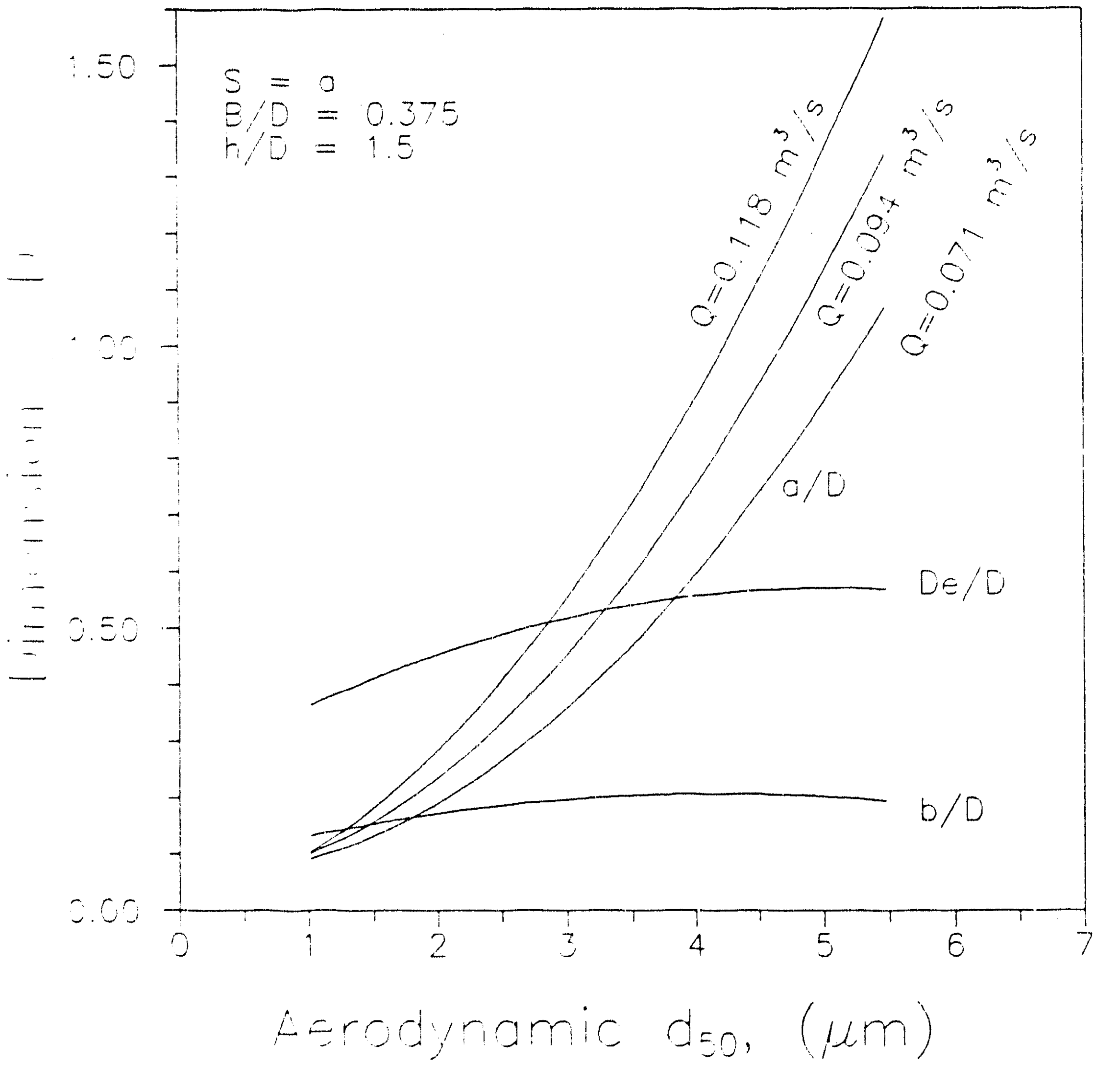

S = a
B/D = 0.375
h/D = 1.5
Q=0.118 m³/s
Q=0.094 m³/s
Q=0.071 m³/s
a/D
De/D
b/D
1.50
1.00
0.50
0.00
0
1
2
3
4
5
6
7
Aerodynamic d50, (μm)

Figure 8.

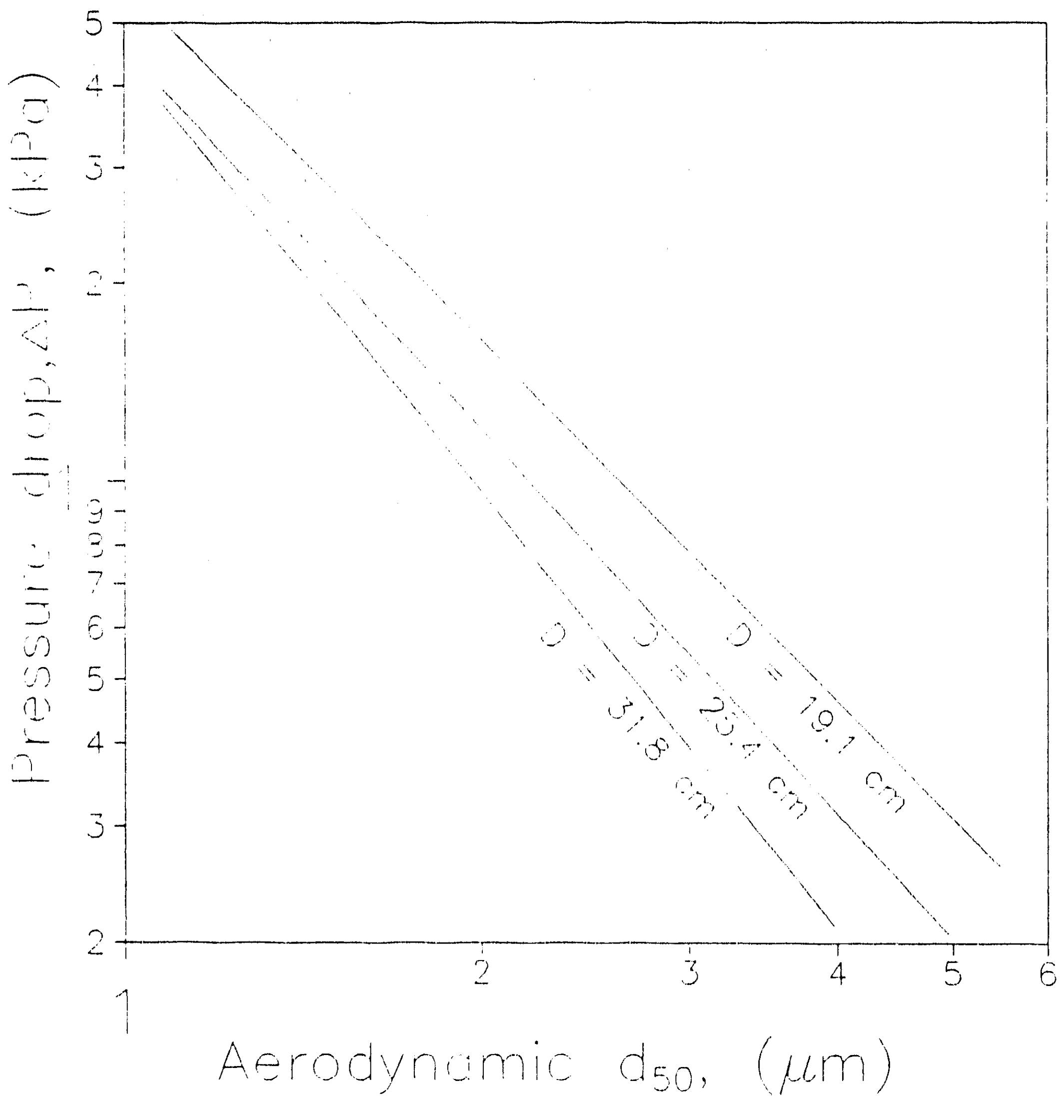

Pressure drop, ΔP, (kPa)
Aerodynamic d_{50}, (μm)
D = 19.1 cm
D = 25.4 cm
D = 31.8 cm

Figure 9.

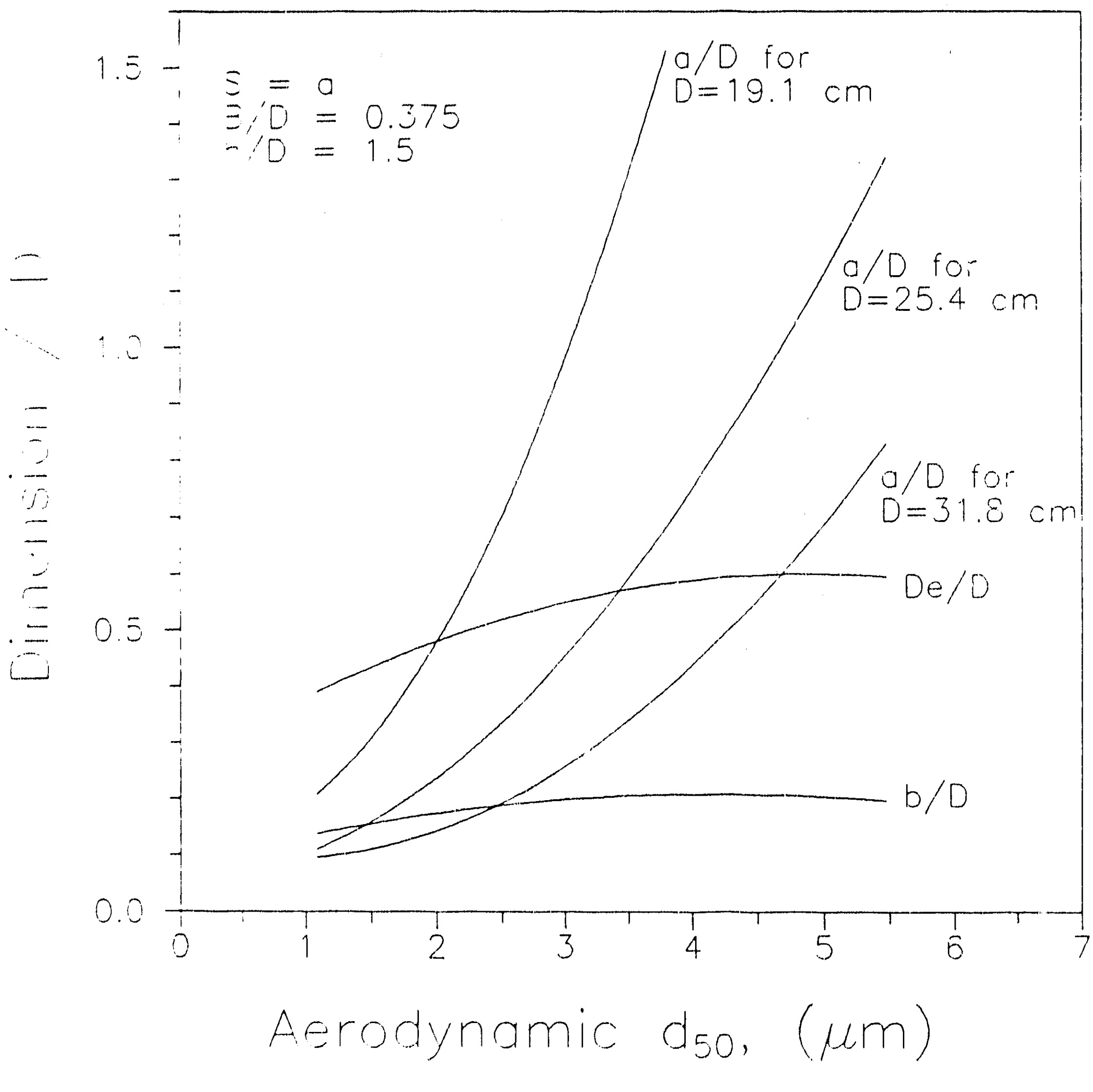
S = a
B/D = 0.375
?/D = 1.5
a/D for D=19.1 cm
a/D for D=25.4 cm
a/D for D=31.8 cm
De/D
b/D
0.0
0.5
1.0
1.5
0
1
2
3
4
5
6
7
Dimension / D
Aerodynamic d_{50}, (μm)

Figure 10

END

DATE FILMED

01 / 04 / 91